Prediction of texture in different beef cuts applying image analysis technique

Facundo Pieniazek
National Council for Scientific and Technical Research, Buenos Aires, Argentina
Agustina Roa Andino
Instituto de Investigaciones Cientificas y Tecnicas para la Defensa, Vicente Lopez, Argentina, and
Valeria Messina
National Council for Scientific and Technical Research, Buenos Aires, Argentina and CITEDEF, Buenos Aires, Argentina

Received 12 December 2017
Revised 8 March 2018
27 May 2018
Accepted 28 May 2018

Abstract

Purpose – Measuring texture parameters are time consuming and expensive; it is necessary to develop an efficient and rapid method to evaluate them. Image analysis can be a useful tool. The purpose of this paper is to predict texture parameters in different beef cuts applying image analysis techniques.
Design/methodology/approach – Samples were analyzed by scanning electron microscopy. Texture parameters were analyzed by instrumental, image analysis techniques and by Warner–Bratzler shear force.
Findings – Significant differences ($p < 0.05$) were obtained for image and instrumental texture features. Higher amount of porous were observed in freeze dried samples of beef cuts from Gluteus Medius and semintendinosus muscles. A linear trend with a linear correlation was applied for instrumental and image texture. High correlations were found between image and instrumental texture features. Instrumental parameters showed a positive correlation with image texture feature.
Originality/value – This research suggests that the addition of image texture features improves the accuracy to predict texture parameter. The prediction of quality parameters can be performed easily with a computer by recognizing attributes within an image.

Keywords Surface analysis techniques, Instrumentation, Quality, Beef cuts
Paper type Research paper

1. Introduction

The variability in meat quality is related to several factors that are spread across the production chain, such as on-farm (breed, diet, and handling), physiological (genetic background, stress, muscle type and location) and processing (post-mortem temperature regime, electrical inputs, storage conditions and cooking). The quality of meat is a multi-dimensional concept where the value of meat and its products are determined based on organoleptic, ethical and social, symbolic and cultural, nutritional and many other factors (Polkinghorne *et al.*, 2008; Herrera-Mendez *et al.*, 2006).

The main source of consumer complaints and/or the most common cause of failure to purchase meat or processed meat are variations in texture (Bekhit *et al.*, 2014; Almli *et al.*, 2013; Chen and Opara, 2013). Texture is a critical factor which has been defined as "all the rheological and structural (geometric and surface) attributes of the product perceptible by means of mechanical, tactile, visual and auditory receptors" (Lawless and Heymann, 1998). It is an important factor associated with food quality; however, a consumer's opinion of texture can vary depending on different factors (Rust *et al.*, 2008).

On the other hand, tenderness is regarded as one of the most important texture attribute that affects the eating quality of meat (Juarez *et al.*, 2012; Powell *et al.*, 2011). Bourne (2002)

British Food Journal

0007-070X
DOI 10.1108/BFJ-12-2017-0695

cited that tenderness is a texture feature. As a texture characteristic it describes a product which, during mastication, displays little resistance to breaking. Due to this, tenderness in meat plays major impact on price of the food (Loebnitz *et al.*, 2015). For example, beef cuts that are known to be tougher (less tender) are marketed at lower prices or even ground and sold as ground beef or utilized in other processed meat. In contrast, those cuts known to be tenderer in texture are sold for much higher premiums as either steaks or roasts (Wezemael and Ueland, 2014; Furnols and Guerrero, 2014).

Multiple instrumental methods have been developed in an attempt to assess the texture of meat, with a focus on tenderness. The main methods currently employed to predict texture parameters are sensory analysis and by instrumental techniques. The former is usually determined by trained or consumer taste panel assessment (Corbin *et al.*, 2015; Savadkoohi *et al.* 2014) while the latter utilizes the Warner–Bratzler shear force (WBSF) method (Fabre *et al.*, 2018; Douglas *et al.*, 2017; Phelps *et al.*, 2016) and by texture profile analysis (TPA) (Isleroglu *et al.*, 2015; Romero de Ávila *et al.*, 2014).

Sensory panel analysis is a subjective evaluation method which heavily reckons on specialized training of taste panel personnel (Sun *et al.*, 2012). They are expensive, time consuming, too cumbersome to be introduced as a routine procedure and not suitable for on-line monitoring (Ghasemi-Varnamkhasti *et al.*, 2010). The response of the panel also has to be properly evaluated because the sensory evaluations varies among panelists; due to that they are individuals with different sensitivities, preferences and product knowledge and within a given panelist fatigue, stress and heath can affect analysis (Meilgaard *et al.*, 1999).

The WBSF, method which was proposed more than half a century ago, can be used to objectively determine mechanical texture profile, such as tenderness in beef. The relationship of instrumental texture variables to the human perception of texture parameters has been a very active area of research, with many researchers addressing this topic (Guzek *et al.*, 2013; Luckett *et al.*, 2016). Therefore, due to the stated points it is necessary to develop an efficient and rapid method to evaluate texture parameters in beef.

An interesting alternative for analyzing texture parameters is to study the surface of food products and appearance characteristics, applying computerized image analysis techniques. Image texture is the perceived changes in scattered light from structural changes in the surface of an object (Russ, 2005). Since Haralick *et al.* (1973) applied Gray Level Co-Occurrence Matrix (GLCM) to the classification of land use categories; there have been numerous applications of the GLCM techniques in different fields (Rojas, 2017; Guangchun *et al.*, 2015; Peng *et al.*, 2014). Several authors have applied multiespectral image analysis to evaluate adulteration of beef and pork in raw meat (Ropodi *et al.*, 2015), assessment of color and aspect evolution in meat (Fongaro *et al.*, 2015); prediction of moisture contents in pork longissimus dorsi muscles (Ma *et al.*, 2015) among others.

The image analysis can be a useful tool for characterizing food morphology because the highly irregular structures of many food materials elude precise quantification by conventional means. Image analysis provides objective evaluations of the morpho-colorimetric features of a sample; it is more quantitative and less biased than the common method of visual perception, which is prone to variation due to the personal opinions of inspectors or trained panels (Kono *et al.*, 2014).

When microscopy techniques such as scanning electron microscopy (SEM) and images analysis are used together, they become a powerful tool to evaluate microstructure changes of a product; cell size and number of cells can them be measured and quantified from the projected image (Barrera *et al.*, 2013). Employing image processing with SEM, some important texture parameters could be predicted by processing the surface and cross-section images of a product (Xue *et al.*, 2017; Kaláb *et al.*, 1995).

The aim of the present research was to predict texture parameters in different freeze dried beef cuts applying image analysis techniques. Data obtained by image analysis were correlated with instrumental analysis in order to evaluate effectiveness of the method.

2. Material and methods

2.1 Samples, cooking process and freeze drying cycle

Semitendinosus (ST) ($n = 4$), Semimembranosus (SM) ($n = 4$), Spinalis Dorsi (SD) ($n = 4$) and Gluteus Medius (GM) ($n = 4$) (sp: Aberdeen Angus) were provided by an abattoir center of Argentina. Animals were feed with pure stands of cereal rye. The small-grain winter annuals were planted in three pastures each that received ten steers randomly allocated from a group of 90 spring born steers of similar age and born weight (551 ± 16.1 days old; 373 ± 17.5 kg).

Preliminary experiments were conducted to test different operative conditions, such as, sample shape, dimension and thickness, method, time of cooking, various procedures to manipulate the sample and freeze drying cycle. The best operating conditions were: whole muscles were cut to about 4 × 2 × 2 cm steaks with the fiber parallel to the longest axis and were individually labeled and weighed. Steaks were grilled in aluminum-folded strips and cooked to an end point temperature of 71.5 ± 0.5°C (AMSA, 1995) using an electric grill (Philips, CABA, Argentina). Internal temperature was monitored with a T-type thermocouple inserted in the geometric center of each steak. Samples were cooled at room temperature (30 min) and then chilled in a refrigerator at 4 ± 1°C for 24 h.

Each cooked (*C*) steak was cut with a cork-bore to a cylindrical form with 13 mm diameter and 3 cm high. The round shape was the best solution to reduce variability caused by lateral sinking. Each cylindrical sample were sliced in units of 1 mm of thickness and stored at 3°C until freeze drying process.

Freeze drying process was carried out in a pilot plant freeze dryer supplied with four trays designed by an Industrial constructor (Rificor, Argentina). Freeze drying cycle was set at −50°C during 24 h and then dried at 40°C during 24 h under a chamber pressure of 0.346 Pa. Samples were packaged, individually identified and stored in a dark place at room temperature until analysis.

In order to analyze microstructure, instrumental and image texture features of cooked freeze dried rehydrated samples (CFDR), rehydration process was performed with tap water at 98 °C. The duration of rehydration process in both muscles was fixed in 6 min, as after that time period there was no more absorption of water by the samples.

2.2 Scanning electron microscopy

SEM was used for the observation of the microstructure of cooked freeze dried (CFD) and CFDR samples of ST, SM, SD and GM. Samples were cross-sectioned using a scalpel; the cut was always performed in the same direction. Samples were mounted on holders and coated with gold (Pieniazek and Messina, 2015). Microscopic evaluation was performed using a scanning electron microscope (SEM 515, Philips, The Netherlands). Observations of the samples at magnification of 250, 500 and 1000 × were obtained for image analysis (Model Genesis Version 5.21.).

Brightness and contrast are the most important variables that must be controlled during the acquisition of images; therefore, the values of these parameters were kept constant for each magnification during the process of image acquisition.

2.3 Measurement of porosity

Porosity (*P*) was performed using a Stereopycnometer (Quantachrome multipycnometer Model MVP-1, USA) with an accuracy of 0.001 cm^3, utilizing helium gas as described by Koc *et al.* (2010).

2.4 Texture Profile Analysis (TPA)

Texture assessment of CST, CGM, CSM, CSD, CFDRSM, CFDRST, CFDRSD and CFDRGM was performed with a texture analyzer (TA-XT-Texture Technologies Corp., UK) with a

5 kg load cell. Measurements were performed using a cylindrical probe SMS P/35 (35 mm diameter) with the following settings: compressed 3 mm with a time interval of 5 s at a speed of 5.0 mm.sec^{-1}, final strain 70 percent and 5 s between the first and second stroke). Results were reported as an average value. Force-by-time data from each test were used to calculate mean values for the TPA parameters. Values for hardness (HAR) (peak force of the first compression cycle in N), cohesiveness (COH) (ratio of the positive force area during the second compression to that during the first compression), springiness (SPRING) (ratio of the time duration of force input during the second compression to that during the first compression) and chewiness (hardness multiplied by cohesiveness multiplied by springiness in N) (Caine *et al.*, 2003).

2.5 Image texture analysis

In total, 18 images (1024 × 800 pixels) were captured of each sample (CST, CGM, CSM, CSD, CFDRSM, CFDRST, CFDRSD and CFDRGM) using a SEM (1,000×) and stored as bitmaps in a gray scale with brightness values between 0 and 255 for each pixel constituting the image. The size of each sample (region of interest: 122 × 122 pixels) was the same for all the evaluated magnifications. Texture parameters were computed from a set of GLCM probability distribution matrices for a given image. The GLCM shows the probability that a pixel of a particular gray level occurs at a specified direction and distance ($d = 1$) from its neighboring pixels. Gray level co-occurrence matrix is represented by Pd,θ (i, j) where counts the neighboring pair pixels with gray values i and j at the distance of d and the direction of θ (Pieniazek and Messina, 2015).

Five image texture features (correlation (COR), energy (ASM), homogeneity (HOM), entropy (ENT) and contrast (CON)) were calculated using MATLAB 8.4. (The MathWorks, Inc., MA, USA):

$$\mathrm{CON} = \sum_{i=0}^{n-1}\sum_{j=0}^{n-1}(i-j)^2 \mathrm{Pd},\theta(i,j), \tag{1}$$

$$\mathrm{ENT} = -\sum_{i=0}^{n-1}\sum_{j=0}^{n-1}\mathrm{Pd},\theta(i,j)^2 \,\mathrm{Log}\, P(i,j), \tag{2}$$

$$\mathrm{HOM} = \sum_{i=0}^{n-1}\sum_{j=0}^{n-1}\frac{\mathrm{Pd},\theta(i,j)}{1+|i-j|}, \tag{3}$$

$$\mathrm{ASM} = \sum_{i=0}^{N-1}\sum_{j=0}^{N-1}\mathrm{Pd},\theta(i,j)^2, \tag{4}$$

$$\mathrm{COR} = \frac{\left[\sum_{i=0}^{N-1}\sum_{j=0}^{N-1}(ij)P(i,j)\right]-\mu_x\mu_y}{\sigma_x\sigma_y}, \tag{5}$$

where u_x, u_y, σ_y and σ_y are the means and standard deviations of p_x and p_y

2.6 Warner–Bratzler Shear Force Measurement (WBSF)

The WBSF protocol measures the amount of force required to shear across entire muscle fibers. This method requires the cooking of the beef to an internal temperature (71°C) and removing at least six 1.27 cm round cross-section cores from throughout the steak after cooling to a consistent temperature, and an instrument cross-head speed of 200–250 mm/min to completely shear cores perpendicular to the muscle fiber orientation (AMSA, 1995).

Therefore, in this research, eight cylinder cores (1.27 cm in diameter and 2.5 ± 0.2 cm in length) were manually and alternately removed parallel to the predominant muscle fiber orientation from each steak. The round cross-section cores were cut out by handling of a cork borer. The Warner–Bratzler shear test was performed using an Instron Universal Testing Machine (Instron, Model 4301, Instron Ltd, UK). The central portion of the core length was positioned under the blade for shearing across the predominant muscle fiber orientation as indicated by WBSF protocol (AMSA, 1995). The cross-head speed was set at 200 mm/min. The average peak shear force of the eight cores was used for the statistical analyses.

2.7 Statistical analysis

Texture and WBSF values were subjected to linear normalization prior to principal component analysis (PCA) in order to efficiently suppress quantitative effects on the multivariate data. Mean values were compared by Student *t*-test ($p < 0.05$), regression equations and correlation coefficients (R^2) between instrumental and image texture features were obtained using SPSS-Advanced Statistics 12 software (SPSS Inc., Chicago, IL).

3. Results

3.1 Scanning electron microscopy

Figure 1 shows microstructure of C, CFD and CFDR samples of GM, SM, ST and SD at 500 × magnifications. CGM, CSM, CST and CSD showed an organized structure with compacted fibers and without gaps. CFDGM, CFDSM, CFDST and CFDSD structures appeared organized showing gaps among fiber bundles and between fibers. Myofibrils were dehydrated and separated and partially fragmented. CFDGM and CFST samples, showed a higher porous size structure with larger and irregular cavities due to ice crystals formed and shrinkage of fiber, when compared to CFDSM and CFSD.

Kiani and Sun (2011) stated that crystallization is a general term used to describe several different phenomena related to the formation of a crystalline lattice structure. This process consists of two main successive stages; nucleation and crystal growth. The interaction between these two steps determines the crystal characteristics, i.e. size, distribution and morphology of the crystals.

Changes in microstructure probably are due to that drying process induced faster denaturation of proteins and subsequently more reduction in dimension of myofibrils and collagen, resulting in shrinkage of muscle fiber diameter and sacromere length (Reyes *et al.*, 2011).

Micrographs of CFRGM, CFRSM, CFRST and CFRSD also showed that due to porous size structure, water easily reoccupied the empty spaces in all samples.

In general, micrographs showed that a higher amount of porous structure were obtained for CFDGM and CFDST, due to ice sublimation during freeze drying process and shrinkage of muscle fiber, when compared to CFDSM and CFDSD.

3.2 Porosity

Significant differences between porosity values ($P < 0.05$) were observed in CFDGM, CFDST, CFDSM and CFDSD. Mean values of CFDGM ($P = 69.76$), CFDST ($P = 67.25$),

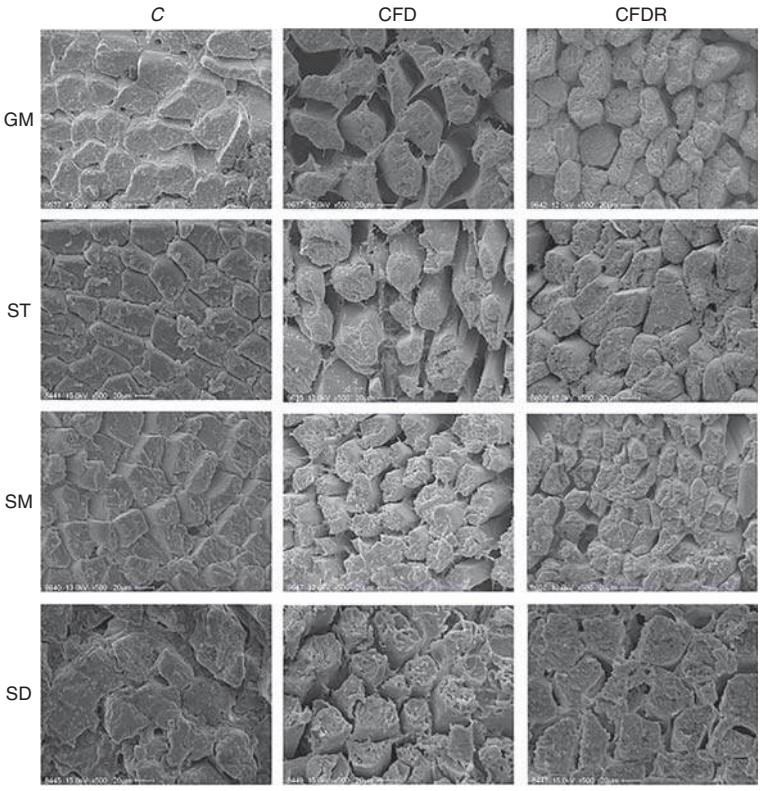

Figure 1.
Scanning micrographs performed at 500X of cross sectional cooked (C), cooked freeze dried (CFD) and cooked freeze dried rehydrated (CFDR) beef cuts of Semitendinosus (ST), Semimembranosus (SM), Spinalis Dorsi (SD) and Gluteus Medius (GM)

CFDSM ($P = 59.9$) and CFDSD ($P = 58.3$), revealed that CFDGM and CFDST had higher porosity when compared to CFDSM and CFDSD.

Porosity in samples depends on different factors, such as cooking parameters, pressure and drying temperature. In freeze drying, high porosity (amounts of pores) helps to maintain the structure without the deformations that are inevitable in other drying methods. The degree of porosity also has influence in texture and rehydration ability, when the size of the air cells in porous material is bigger; it allows a fast rehydration due to that water easily enters and reoccupies the empty spaces (Oikonomopoulou *et al.*, 2011). During subsequent freezing and freeze drying, the ice sublimation creates pores; the amount of pores (porosity) is related to the water uptake and is higher when the water uptake is increased.

When porosity was related to SEM images, results showed that CFDGM and CFDST had higher porosity. Due to the high porosity, the freeze dried cell suspension has a high-specific surface area; this influences the sorption behavior as well as the rehydration. Therefore, SEM micrographs with porosity confirm the based microstructure discussion presented above.

3.3 Image texture analysis

Table I shows image texture values for CST, CGM, CSM, CSD, CFDRST, CFDRGM, CFDRSD and CFDRST at 1000 X magnification. Significant differences ($P < 0.05$) for ASM, CON, ENT, COR, and HOM were obtained for C and CFDR samples.

Sample	Image texture				
	ASM	ENT	CON	COR	HOM
CST	0.29[b]	6.53[a]	0.64[b]	0.81[b]	0.91[b]
CFDRST	0.70[a]	4.83[b]	0.70[a]	0.93[a]	0.94[a]
p-value	0.0001	0.0001	0.0001	0.0001	0.0001
CGM	0.86[b]	6.80[a]	0.88[b]	0.92[b]	0.95[b]
CFDRGM	0.99[a]	5.35[b]	0.94[a]	0.95[a]	0.97[a]
p-value	0.0056	0.0001	0.0001	0.0051	0.0054
CSM	0.35[b]	6.15[a]	0.55[b]	0.78[b]	0.85[b]
CFDRSM	0.57[a]	5.26[b]	0.65[a]	0.86[a]	0.98[a]
p-value	0.0001	0.0001	0.0001	0.0001	0.0001
CSD	0.45[b]	6.25[a]	0.43[b]	0.75[b]	0.83[b]
CFDRSD	0.68[a]	5.49[b]	0.55[a]	0.86[a]	0.97[a]
p-value	0.0001	0.0001	0.0001	0.0001	0.0001

Notes: CST, cooked Semintendinosus; CGM, cooked Gluteus Medius; CSM, cooked Semimembranosus; CSD, cooked Spinalis Dorsi; CFDRST, cooked freeze dried rehydrated Semintendinosus; CFDRGM, cooked freeze dried rehydrated Gluteus Medius, CFDRSM, cooked freeze dried rehydrated Semimembranosus; CFDRSD, cooked freeze dried rehydrated Spinalis Dorsi; ASM, energy; ENT, entropy; CON, contrast; COR, correlation; HOM, homogeneity. [a,b]indicate that means are significantly different ($p < 0.05$) related to treatment (*t*-student)

Table I. Image texture values of cooked and cooked freeze dried rehydrated Semitendinosus, Gluteus Medius, Semimembranosus and Spinalis Dorsi bovine muscles (Sp: aberdeen angus)

In texture image analysis, COR indicates the linearity of the image. For an image with large areas of similar intensities, a high value of correlation is measured. HOM shows the level of uniformity on the image. High values of HOM show improvement of uniformity and smoothness of the image (Karimi *et al.*, 2012). ENT is a measure of randomness, and takes low values for smooth images.

ASM represents the smoothness of an image, when ASM is high the image has very similar pixels. CON is a measure that shows the difference from one pixel to others close to it. It is a measure of local gray variations. Low values in CON represent diminish of local variation of pixels. The softer the texture the lower the contrast, which is due to lower pixel value difference between two neighbors. Higher values of ENT; lower values of ASM, COR, HOM and CON were obtained in *C* when compared to CFDR.

CFDR samples showed to be homogeneous, a better correlation among neighboring pixel was obtained, higher degree of local variations appeared, and high linearity and roughness appeared; when compared to *C* samples. The use of magnified images increases prediction accuracy on texture features and reduces computation time.

On the other hand, CON values are related to softness and toughness, higher values of CON are related to toughness; lower values to softness. Results revealed that CON values in CFDR were slightly higher than *C* samples. Hardness probably increased due to freeze drying process. In general results revealed that toughness appeared in CFDRGM muscles followed by CFDRST; predicting softness in CFDRSM followed by CFDRSD muscles.

3.4 Instrumental texture analysis

Table II shows texture values of *C* and CFDR samples of ST, GM, SM and SD. Statistical difference ($p < 0.0001$) was obtained for CHEW, HARD, COH, and SPRIN in muscles. Results revealed that CFDR samples were harder than C in the samples. Hardness appeared in CFDRST followed by CFDRGM; CFDRSD and CFDRSM revealed lower values of hardness.

3.5 Correlation between instrumental and image texture

In order to evaluate the capability of instrumental and image analysis for texture, a linear trend with a linear correlation under evaluated conditions were analyzed with instrumental

Sample	Instrumental texture			
	HARD	SPRING	COH	CHEW
CST	67.79[b]	0.44[b]	0.50[b]	16.72[b]
CFDRST	69.82[a]	0.47[a]	0.54[a]	17.89[a]
p-value	0.0001	0.0001	0.0001	0.0001
CGM	71.35[b]	0.51[b]	0.49[b]	18.31[b]
CFDRGM	72.35[a]	0.55[a]	0.52[a]	19.10[a]
p-value	0.0001	0.0001	0.0001	0.0001
CSM	58.23[b]	0.42[b]	0.63[b]	20.64[b]
CFDRSM	62.30[a]	0.45[a]	0.66[a]	22.05[a]
p-value	0.0001	0.0001	0.0001	0.0001
CSD	41.93[b]	0.43[b]	0.57[b]	10.56[b]
CFDRSD	44.20[a]	0.46[a]	0.61[a]	13.25[a]
p-value	0.0001	0.0001	0.0001	0.0001

Notes: CST, cooked Semintendinosus; CGM, cooked Gluteus Medius; CSM, cooked Semimembranosus; CSD, cooked Spinalis Dorsi; CFDRST, cooked freeze dried rehydrated Semintendinosus; CFDRGM, cooked freeze dried rehydrated Gluteus Medius, CFDRSM, cooked freeze dried rehydrated Semimembranosus; CFDRSD, cooked freeze dried rehydrated Spinalis Dorsi; HARD, hardness; SPRING, springiness; COH, cohesiviness; CHEW, chewiness. [a,b]indicate that means are significantly different ($p < 0.05$) related to treatment (*t*-student)

Table II. Instrumental texture values for cooked and cooked freeze dried rehydrated Semitendinosus, Gluteus Medius, Semimembranosus and Spinalis Dorsi bovine muscles (Sp: aberdeen angus)

(CHEW, COH, SPRING, and HARD) vs image features (ASM, CON, ENT, COR, and HOM) of C and CFDR samples.

PCA was performed for each texture parameters (instrumental and image). Two PC's were found for instrumental texture for each beef cut accounting 95.6 percent (CST and CFDRST), 91.2 percent (CGM and CFDRGM), 94.7 percent (CSM and CFDSM) and 91.8 percent (CSD and CFDRSD) of the total variance; two PC's were found for image texture for each beef cut accounting 90.5 percent (CST and CFDRST), 89.8 percent (CGM and CFDRGM), 92.3 percent (CSM and CFDRSM) and 90.7 percent (CSD and CFDRSD) of the total variance. Each PC score was multiplied by the respective variance. PC_1 of instrumental and image texture were combined using a linear combination.

Figure 2 shows linear trend with a linear correlation of PCA scores of texture parameters (instrumental vs image texture) of *C* and CFDR samples. Results revealed a strong relationship between instrumental and image features for *C* and CFDR samples (ST ($R = 0.946$), SM ($R = 0.905$), GM ($R = 0.937$) and SD ($R = 0.938$)) based on the resulting R^2 value, the model explained 92.0, 87.0, 89.3 and 89.3 percent, respectively, of the variability that associated with instrumental with image features.

3.6 TPA and WBSF

WBSF values between 31.38 and 38.25 N were used as cut-off values for very tender and tender beef, respectively (Sullivan and Calkins, 2011). Mean values of WBSF of CFDR samples (CFDST = 37.91 N; CFDGM = 36.25 N; CFDSM = 34.51 N; CSFDD = 33.51) were higher than *C* samples (CST = 36.53 N; CGM = 34.39 N; CSM = 33.12 N; CSFDD = 31.9). CST, CFDRST, CGM and CFDRGM showed higher WBSF values when compared to CSM, CFDRSM, CSD and CFDRSD samples. In order to correlate image with instrumental texture features, values for WBSF between 31.0 and 39.0 N were used as cut-off values for tenderness.

PCA was applied for image texture features and WBSF data. Two PC's (*C* and CFDR) were obtained for each beef cut explaining 98.2 (CST and CFDRST), 97.7 (CGM and CFDRGM), 96.5 (CSD and CFDRSD) and 97.3 percent CSM and CFDRSM) of the total variance (data not shown).

Results revealed that CON values in *C* and CFDR were positively correlated with WBSF. Image texture features extracted from the full images predicted WBSF scores with an

R^2 value of 0.5 and correctly classified them into categories of "very tender" and "tender" with an 83 percent success rate. Features extracted from the close-up images predicted WBSF scores with an R^2 value of 0.83 and classified them with a 93 percent success rate. Among these texture features evaluated, results revealed that ST (*C* and CFDR) was tougher (less tender) than GM (*C* and CFDR); followed by SM (*C* and CFDR) and SD (*C* and CFDR). Among beef cuts, SD (*C* and CFDR) showed to be "very tender" when compared to other beef cuts.

Ruiz de Huidobro *et al.* (2005) reported that tenderness can be predicted in beef because the meat tissue characteristics that influence meat quality and the connective tissue quantity and spatial distribution that define the grain of meat are directly related to it. Overall, these results suggested that the CON texture features extracted from images analysis could be very useful to evaluate tenderness (texture parameter).

3.7 Limitation of the study

The limitations of this study are that prediction of texture parameters with image analysis techniques in different beef cuts will be valid and reliable only for those beef cuts that are very similar to the sample on which the instrument's validity and reliability were originally established. It is necessary to analyze a higher number of animals, different type of breed, age, diet and pseudo-repetitions to improve the research.

4. Conclusions

An imaging-based technique was developed to approach texture properties in different beef cuts. Image texture analysis had high correlations with instrumental texture features. On the other hand, images of beef surface allowed classifying beef in terms of texture parameter.

These results suggest that the addition of image texture features significantly improves the accuracy to predict texture parameters, due to that the prediction of texture can be performed easily as a quantitative technique that could be related in future studies for quality. Anyway, it would be recommendable to study other beef cuts in future research to improve research and to establish a general trend.

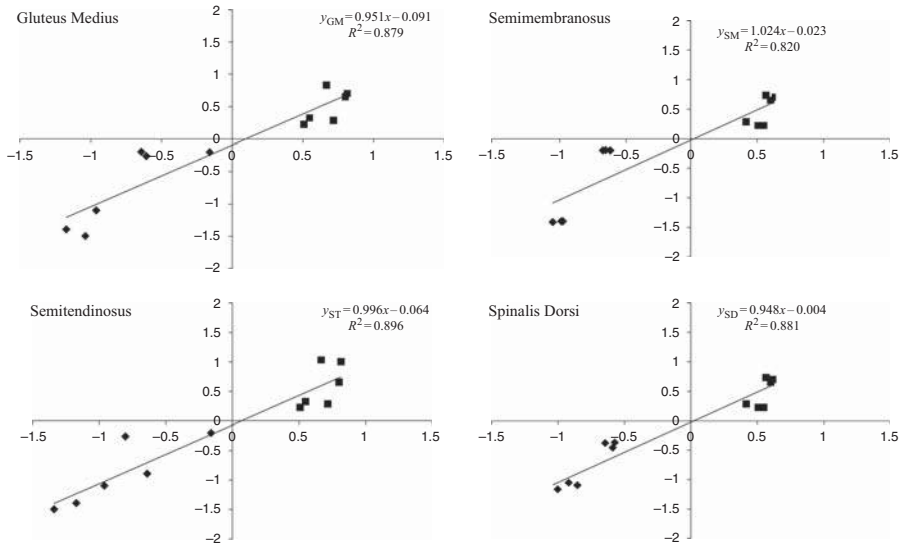

Figure 2. Correlation coefficients of PCA scores between instrumental texture vs image texture of cooked (▲) and cooked freeze dried rehydrated (■) beef cuts of Semitendinosus (ST), Semimembranosus (SM), Spinalis Dorsi (SD) and Gluteus Medius (GM)

References

Almli, V., Wezemael, V., Verbeke, L. and Uelan, O. (2013), "One technology does not fit all: profiling consumers of tender and tenderized beef steaks", *Meat Science*, Vol. 93, pp. 361-370.

AMSA (1995), *Research Guidelines for Cookery, Sensory Evaluation, and Instrumental Tenderness Measurements of Fresh Meat*, American Meat Science Association (AMSA) & National Live Stock and Meat Board, Chicago.

Barrera, G., Calderón-Domínguez, G., Chanona-Pérez, J., Gutiérrez-López, G., León, A. and Ribotta, P. (2013), "Evaluation of the mechanical damage on wheat starch granules by SEM, ESEM, AFM and texture image analysis", *Carbohydrate Polymers*, Vol. 98, pp. 1449-1457.

Bekhit, A., Carne, A., Ha, M. and Frank, F. (2014), "Physical interventions to manipulate texture and tenderness of fresh meat: a review", *International Journal of Food Properties*, Vol. 17, pp. 433-453.

Bourne, M. (2002), *Food Texture and Viscosity: Concept and Measurement*, Academic Press, New York, NY.

Caine, W., Aalhus, J., Best, D., Dugan, M. and Jeremiah, L. (2003), "Relationship of texture profile analysis and Warner-Bratzler shear force with sensory characteristics of beef rib steaks", *Meat Science*, Vol. 64, pp. 333-339.

Chen, L. and Opara, U. (2013), "Approaches to analysis and modeling texture in fresh and processed foods – a review", *Journal of Food Engineering*, Vol. 119, pp. 497-507.

Corbin, C., O'Quinn, T., Garmyna, A., Legako, J., Hunt, M., Dinh, T., Rathmann, R., Brooks, J. and Miller, M. (2015), "Sensory evaluation of tender beef strip loin steaks of varying marbling levels and quality treatments", *Meat Science*, Vol. 100, pp. 24-31.

Douglas, R., Silva, De Moura, A., Alcinéia, L. and Ramos, E. (2017), "Comparison of Warner-Bratzler shear force values between round and square cross-section cores for assessment of beef Longissimus tenderness", *Meat Science*, Vol. 125 No. 1, pp. 102-105.

Fabre, R., Dalzotto, G., Perlo, F., Bonato, P., Teira, G. and Tisocco, O. (2018), "Cooking method effect on Warner-Bratzler shear force of different beef muscles", *Meat Science*, Vol. 138, pp. 10-14.

Fongaro, L., Alamprese, C. and Casiraghi, E. (2015), "Ripening of salami: assessment of colour and aspect evolution using image analysis and multivariate image analysis", *Meat Science*, Vol. 101, pp. 73-77.

Furnols, M. and Guerrero, L. (2014), "Consumer preference, behavior and perception about meat and meat products: an overview", *Meat Science*, Vol. 98, pp. 361-371.

Ghasemi-Varnamkhasti, M., Saeid Mohtasebi, S. and Siadat, M. (2010), "Biomimetic-based odor and taste sensing systems to food quality and safety characterization: an overview on basic principles and recent achievements", *Journal of Food Engineering*, Vol. 100, pp. 377-387.

Guangchun, G., Shengying, Z., Cui, Z., Xiaobin, Y. and Ziqiao, L. (2015), "Study on fruit recognition methods based on compressed sensing", *Journal of Computational and Theoretical Nanoscience*, Vol. 12, pp. 2937-2942.

Guzek, D., Głąbska, D., Pogorzelska, E., Pogorzelski, G. and Wierzbick, A. (2013), "Instrumental measurement of meat in a laboratory research and on a production line", *Advances in Science and Technology Research Journal*, Vol. 7, pp. 5-11.

Haralick, R., Shanmuham, K. and Dinstein, I. (1973), "Texture features for image classification", *Transaction on Systems, Man and Cybernetic*, Vol. 3, pp. 610-621.

Herrera-Mendez, C., Becila, S., Boudjellal, A. and Ouali, A. (2006), "Meat ageing: reconsideration of the current concept", *Trends in Food Science and Technology*, Vol. 17, pp. 394-405.

Isleroglu, H., Kemerli, T. and Kaymak-Ertekin, F. (2015), "Effect of steam-assisted hybrid cooking on textural quality characteristics, cooking loss, and free moisture content of beef", *International Journal of Food Properties*, Vol. 18, pp. 403-414.

Juarez, M., Aldai, N., Lopez-Campos, O., Dugan, M., Uttaro, B. and Aalhus, J. (2012), "Beef texture and juiciness", in Hui, Y.H. (Ed.), *Handbook of Meat and Meat Processing*, CRC Press, Boca Raton, FL, pp. 177-206.

Kaláb, M., Allan-Wojtas, P. and Shea Miller, S. (1995), "Microscopy and other imaging techniques in food structure analysis", *Trends in Food Science and Technology*, Vol. 6, pp. 177-186.

Karimi, M., Fathi, M., Sheykholeslam, Z., Sahraiyan, B. and Naghipoor, F. (2012), "Effect of different processing parameters on quality factors and image texture features of bread", *Journal of Bioprocess and Biotechnology*, Vol. 2 No. 3, pp. 12-17.

Kiani, H. and Sun, D. (2011), "Water crystallization and its importance to freezing of foods: a review", *Trends in Food Science & Technology*, Vol. 22 No. 8, pp. 407-426.

Koc, B., Sakin, M., Balkir, P. and Kaymak-Ertekin, F. (2010), "Spray drying of yoghurt: optimization of process conditions for improving viability and other quality attributes", *Drying Technology*, Vol. 28 No. 4, pp. 495-507.

Kono, S., Kawamura, I., Yamagami, S., Araki, T. and Sagara, Y. (2014), "Optimum storage temperature of frozen cooked rice predicted by ice crystal measurement, sensory evaluation and artificial neural network", *International Journal of Refrigeration*, Vol. 56 No. 1, pp. 165-172.

Lawless, H. and Heymann, H. (1998), *Sensory Evaluation of Food: Principals and Practices*, Chapman and Hall, New York, NY.

Loebnitz, N., Mueller Loose, S. and Grunert, K. (2015), "Impacts of situational factors on process attribute uses for food purchases", *Food Quality and Preference*, Vol. 44 No. 3, pp. 84-91.

Luckett, C., Kuttappan, V., Johnson, L., Owens, C. and Seo, H. (2016), "Comparison of three instrumental methods for predicting sensory attributes of poultry deli meat", *Journal of Sensory Studies*, Vol. 29 No. 1, pp. 171-181, available at: https//doi:10.1111/joss.12092

Ma, J., D-Wen, S. and Hong, P. (2015), "Spectral absorption index in hyperspectral image analysis for predicting moisture contents in pork longissimus dorsi muscles", *Food Chemistry A*, Vol. 197 No. 6, pp. 848-854.

Meilgaard, M., Carr, B. and Civille, G. (1999), *Sensory Evaluation Technique*, 3rd ed., CRC Press, Boca Raton, FL.

Oikonomopoulou, V., Krokida, M. and Karathanos, V. (2011), "The influence of freeze drying conditions on microstructural changes of food products", *Procedia Food Science*, Vol. 1 No. 1, pp. 647-654.

Peng, H., Xiaoqing, W., Chenglin, W. and Yingpu, J. (2014), "Determination of animal oil added in vegetable oil by standard chemical method coupled with image texture analysis technology", *International Journal of Innovative Computing, Information and Control*, Vol. 10 No. 4, pp. 67-80.

Phelps, K., Drouillard, J., Silva, M., Miranda, L., Ebarb, S., Van Bibber-Krueger, C., O'Quinn, T. and Gonzalez, J. (2016), "Effect of extended postmortem aging and steak location on myofibrillar protein degradation and Warner-Bratzler shear force of beef M. Semitendinosus steaks", *Journal of Animal Science*, Vol. 94 No. 1, pp. 412-423.

Pieniazek, F. and Messina, V. (2015), "Textura and color analysis of lentil and rice for instant meal using image processing techniques", *International of Food Processing and Preservation*, Vol. 40 No. 1, pp. 969-978.

Polkinghorne, R., Philpott, D., Gee, A., Doljanin, A. and Innes, J. (2008), "Development of a commercial system to apply the meat standards Australia grading model to optimize the return on eating quality in a beef supply chain", *Australian Journal of Experimental Agriculture*, Vol. 48 No. 2, pp. 1451-1458.

Powell, L., Nicholson, K., Huerta-Montauti, D., Miller, R. and Savell, J. (2011), "Constraints on establishing threshold levels for Warner-Bratzler shear-force values based on consumer sensory ratings for seven beef muscles", *Animal Production Science*, Vol. 51 No. 10, pp. 959-966.

Reyes, A., Perez, N. and Mahn, A. (2011), "Theoretical and experimental study of freeze drying 'loco' (Concholepas concholpeas)", *Drying Technology*, Vol. 29 No. 12, pp. 1386-1395.

Rojas, N. (2017), "Weed recognition by SVM texture feature classification in outdoor vegetable crop images", *Investigacion Agraria*, Vol. 37 No. 6, pp. 68-74.

Romero de Ávila, D., Isabel Cambero, M., Ordóñez, J., De la Hoz, L. and Herrero, A. (2014), "Rheological behaviour of commercial cooked meat products evaluated by tensile test and texture profile analysis (TPA)", *Meat Science*, Vol. 98 No. 2, pp. 310-315.

Ropodi, A., Pavlidisa, D., Mohare, F., Panagoua, E. and Nychasa, G. (2015), "Multispectral image analysis approach to detect adulteration of beef and pork in raw meat", *Food Research International*, Vol. 67 No. 1, pp. 12-18.

Ruiz de Huidobro, F., Miguel, E., Blázquez, B. and Onega, E. (2005), "A comparison between two methods (Warner-Bratzler and texture profile analysis) for testing either raw meat or cooked meat", *Meat Science*, Vol. 69 No. 3, pp. 527-536.

Russ, J. (2005), "The need for stereology", *Image Analysis of Food Microstructure*, CRC LLC, Taylor and Francis, Boca Raton, FL, pp. 1-20.

Rust, S., Price, D., Subbiah, J., Kranzler, G., Hilton, G., Vanoverbeke, D. and Morgan, J. (2008), "Predicting beef tenderness using nearinfrared spectroscopy", *Journal of Animal Science*, Vol. 86 No. 2, pp. 211-219.

Savadkoohi, S., Hoogenkamp, H., Shamsic, K. and Farahnaky, A. (2014), "Color, sensory and textural attributes of beef frankfurter, beef ham and meat-free sausage containing tomato pomace", *Meat Science*, Vol. 97 No. 4, pp. 410-418.

Sullivan, G. and Calkins, C. (2011), "Ranking beef muscles for Warner-Bratzler shear force and trained sensory panel ratings from published literature", *Journal of Food Quality*, Vol. 34 No. 3, pp. 195-203.

Sun, X., Chen, K., Maddock-Carlin, k., Anderson, V., Lepper, A., Schwartz, C., Keller, W., Ilse, B., Magolski, J. and Berg, A. (2012), "Predicting beef tenderness using color and multispectral image texture features", *Meat Science*, Vol. 92 No. 4, pp. 386-393.

Wezemael, L. and Ueland, O. (2014), "Relationships between sensory evaluations of beef tenderness, shear force measurements and consumer characteristics", *Meat Science*, Vol. 97 No. 3, pp. 310-315.

Xue, S., Wang, H., Yang, H., Yu, X., Bai, Y., Xu, X. and Ma, H.G. (2017), "Effects of high-pressure treatments on water characteristics and juiciness of rabbit meat sausages: role of microstructure and chemical interactions", *Innovative Food Science & Emerging Technologies*, Vol. 41 No. 1, pp. 150-159.

Corresponding author
Valeria Messina can be contacted at: vmessina@citedef.gob.ar